Research Journal of Applied Sciences, Engineering and Technology 7(24): 5234-5241, 2014
DOI:10.19026/rjaset.7.919
ISSN: 2040-7459; e-ISSN: 2040-7467

Submitted: February 22, 2014 Accepted: March 20, 2014 Published: June 25, 2014

Research Article

Challenges in Detection of High Impedance Faults on Broken Conductors in MV Lines

[1]Yasin Khan, [1]Faisal Rehman Pazheri, [2]Sami Ghannam, [1]Abdulrehman Ali Al-Arainy and [1]Nazar Hussain Malik
[1]Department of Electrical Engineering, College of Engineering, Saudi Aramco Chair in Electrical Power, King Saud University, P.O. Box 800, Riyadh-11421, Saudi Arabia
[2]Department of Consulting Services, Saudi Aramco, Dammam, Saudi Arabia

Abstract: The weather conditions in Saudi Arabia are harsh and the inland areas are very hot, dry and sandy. Thousands of kilometers of medium voltage overhead lines (13.8 kV) are located in deep desert areas feeding loads that are located in remote desert areas. Such medium and low voltage distribution networks face difficulties regarding fault detection and localization. High Impedance Fault (HIF) resulting from a broken conductor in MV overhead lines represent the most challenging problem in such environments. Such condition may cause damage, fire or electric shock hazards resulting in life threatening situations. This study reports on a study of electrical characteristics of inland desert sand and typical characteristics of HIF fault when a MV line conductor breaks and touches such sand. It is shown that the arid desert sand has extremely high resistivity and it is difficult to detect the fault by using conventional protective devices. The study presents results of measurements and simulations and suggests that innovative approaches have to be employed to achieve the desired protection in such environments.

Keywords: Desert sand, grounding, high impedance fault, MV distribution system, soil resistivity

INTRODUCTION

Power transmission and distribution systems constitute vital links that provide the continuity of service from the generating stations to the end users. The overhead line conductors of such systems are prone to physical contact with the neighboring objects such as trees, buildings, or surface below them. The detection of such situations is an important issue which currently exists in the electric power utilities (Aucoin and Jones, 1996; Jincheng and Jeffery, 1999; Senger *et al*., 2000). Hence, providing with the proper and fast protection methodologies is quite essential for the safe and reliable operation of power systems in such environments.

Power system protection devices basically aim to detect the occurrence of a fault in order to initiate the correct tripping action to isolate the minimized faulted area as rapidly as possible (Craig, 2001; Callhoun *et al*., 1982). This is done in order to avoid the equipment and property damage and to ensure the service continuity and personnel safety. Delayed relay operation or mal-function can increase the risk of equipment damage, loss of life and can cause supply interruptions (Lee, 1982). However, due to complexities of large networks, traditional relaying algorithms may sometimes be inadequate. Historically and up to recent years, research on HIF mitigation was mainly directed on devices approach or relaying protection algorithms. With emergence of Smart Grid, focus is shifting towards more advanced protection techniques employing technologies such as modern signal processing, communications facilities and intelligent elements. Such tools are increasingly being used for the next generation of relaying and protection systems. Also, other supplementary schemes such as fault localization are becoming increasingly important (Russel, 1988a, b; Sultan and Swift, 1994; IEEE PSRC Working Group D15, 2000; Aucoin, 1982, 1987; Girgis *et al*., 1990; David *et al*., 1998; Lai *et al*., 2005; Samantaray *et al*., 2008; Salam, 2012a, b; Salam and Noh, 2012; Salam and Morsidi, 2010).

High Impedance Faults (HIF) is usually caused when a current carrying conductor inadvertently makes a temporary contact with the ground or is temporarily short-circuited with another current carrying conductor through a highly resistive material. The resulting fault current is usually lower than the nominal current of the system. Typical fault currents for MV 13.8 kV distribution feeders are given in Table 1 (Aucoin and Jones, 1996). For dry sand the fault current is almost zero. The weather conditions in Saudi Arabia are harsh and the inland areas are very hot, dry and sandy. Thousands of kilometers of medium voltage overhead lines (13.8 kV) are located in deep desert areas. A down and broken conductor in such an environment is usually very difficult to detect. As compared to high and extra-

Corresponding Author: Yasin Khan, Department of Electrical Engineering, College of Engineering, Saudi Aramco Chair in Electrical Power, King Saud University, P.O. Box 800, Riyadh-11421, Saudi Arabia

Table 1: Typical fault currents on various surfaces (Aucoin and Jones, 1996)

Surface	Current at 13.8 kV
Dry asphalt	0
Concrete (non-reinforced)	0
Dry sand	0
Wet sand	15
Dry sod	20
Dry grass	25
Wet sod	40
Wet grass	50
Concrete (reinforced)	75

high voltage systems, medium and low voltage distribution networks face challenging situations regarding the fault detection and localization.

Due to reasons mentioned above, conventional over current protection devices are usually not able to detect the existence of HIF and thus HIF resulting from downed conductors represent the most challenging problem at medium voltage levels in high resistivity soils. Such condition may cause damage, fire or electric shock hazards. The failure of HIF detection can be life threatening for humans and livestock. In such cases, the grounding installation design becomes very challenging. In earlier work, the authors proposed an effective method of calculating optimum ground pit dimensions by using low resistivity materials in high resistivity soils in order to reduce its equivalent grounding resistance to an acceptable limit (Al-Arainy *et al*., 2011a, b; Khan *et al*., 2010, 2012).

The aim of this study is to investigate the electrical characteristics of inland loose desert sand in order to examine its implications for the MV distribution system protection. For this purpose, experimental investigations were carried out to study the electrical characteristics of some selected desert sand samples. A detailed experimental and theoretical study was carried out considering different parameters that can influence the protection and the results are summarized in this study.

EXPERIMENTAL SETUP AND METHOD

In order to measure the resistivity of loose sand, a test cell was designed and fabricated. This cell consisted of an insulating tube with two brass flanges connected at each end as shown in Fig. 1. For

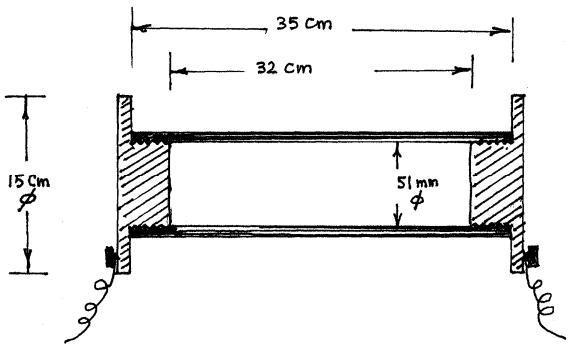

Fig. 1: Test cell used to measure the sand resistivity

measurements of sand resistivity, the test cell was filled with the selected sand sample and the two flanges were then tightened up to hold the sand sample in between the electrodes without any gaps. The resistance between the two flanges was measured with a precise Megger with sand filled in the cell (R_1) as well as without any sand in the test cell (R_2). It was found that $R_1 >> R_2$. Thus R_1 effectively represents resistance of sand particles between the electrodes. The resistivity of sand particles was then determined using the well known relation:

$$\rho = R_1 A / l \quad (1)$$

where,

R_1 = Resistance of sand sample in sand resistivity in π (ohms)
A = Internal area of the tube (m^2)
l = Length of the tube filled with sand (m)
δ = Sand resistivity in (π - m)

For the test cell used, the Eq. (1) becomes:

$$\delta = 6.133 \times 10^{-3} R_1 \text{ (.m)} \quad (2)$$

In the medium voltage distribution network system, the upstream (sending-end) detection is usually based on the signals measured at the distribution substation. Such current and voltage signals depend on the instrument transformers used, grounding arrangement employed as well as the soil resistivity.

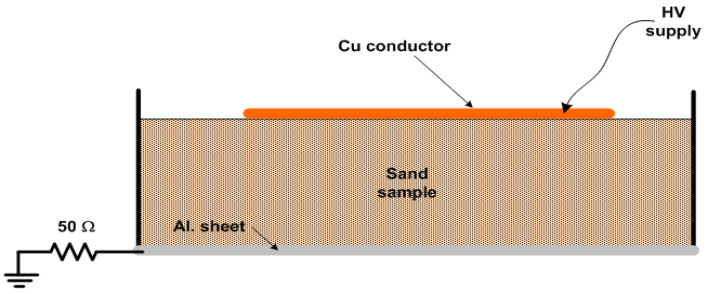

Fig. 2: Schematic diagram of the test setup

In order to study the nature of the fault currents in the medium voltage distribution system with live conductor in contact with the sand, an experimental setup shown in Fig. 2 was prepared in the High Voltage Laboratory and the effects of different parameters such as sand layer thickness and applied voltage type and magnitude, etc., on the resulting fault current were studied. For a specified sand layer thickness, both DC and AC applied voltages were used and the corresponding current flow to the earth was measured using a 50 Ω detection resistance and an oscilloscope (Tecktronics-320). The results for different measurements are presented in the following sections.

RESULTS AND DISCUSSION

Experimental results: In order to confirm the simulated results and to study the actual electrical characteristics of the sample of the loose drifting sand was collected from the inland arid desert near Riyadh, Saudi Arabia and investigated. The following characteristics were found.

Sand resistivity: For testing and calibration purposes, some samples of known resistivity were initially tested using the test cell shown in Fig. 1. After verifying the accuracy of the method, several desert sand samples were studied. The resistivity measurements were made under different applied voltage levels. Based on the average value of the measured sand resistance, it was concluded that the tested samples of loose desert sand had resistivity (ρ) of the order of MΩ-m.

A special test cell of 10 cm diameter similar to one shown in Fig. 1 with one movables electrode was also used to study the effect of pressure or compaction on the resistivity of loose desert sand. The results for one type of sand samples are shown in Table 2. These results indicate that the resistivity of the sand sample decreases with an increase in applied pressure. For loose sand $\rho = 12.74\times10^6$ Ωm. However under pressure of about 2 metric tons, it decreases many folds to a constant value of about 1.76×10^6 Ωm. Similar, behavior was noticed for other sand samples as well. Thus, drifting and loose desert sand exhibits extremely high resistivity and is the main reason for HIF situations in such desert areas. In the inland deserts, storms are common and drifting sand layer usually covers the area. Such sand layers have very high ρ values.

Fault resistance calculations: If an energized overhead line conductor falls on ground, a layer of loose sand exists between the high voltage conductor and the compact soil layer underneath. If one assumes that the compact soil under the drifting sand layer is a perfect conductor with zero resistivity and the total fault resistance is due to the sand layer only, it is possible to get an idea about the possible values of the fault

Table 2: Variations in the sand layer resistance and resistivity with pressure*

Pressure (M. tons)	Sand layer thickness (cm)	Resistance (M Ω)	Resistivity (M Ω-m)
0.00	10.00	150	12.74
0.25	9.90	35	3.00
0.50	9.80	30	2.60
0.75	9.75	26	2.27
1.00	9.70	24	2.10
1.25	9.65	22	1.94
1.50	9.65	20	1.76
2.00	9.65	20	1.76

*: Test cell details: Length (L) = 11.3 cm; Cell diameter (d) = 10 cm

Table 3: Measured and calculated values of sand layer resistance

Sand layer thickness (cm)	Resistivity (MΩ)	
	Measured	Calculated
2	24	27.6
4	40-45	49
6	60-70	62
8	70-75	71
10	85-95	78

resistance. Obviously, this will depend on the sand resistivity and the surface area of the conductor in contact with the sand. Assume that a conductor of length L and radius r is lying on the sand and makes an angle of contact θ with the d layer as shown in Fig. 3. Consider a layer of soil w i^{th} thickness dx located at a distance x from the top. Let us assume that the sand layer of thickness t is solidly earthed at the bottom as shown in Fig. 2. The leakage current passing through this layer of thickness dx and having a cross-sectional area A will lead to sa fault resistance dR_g. The expression for this fault or earth resistance (dR_g) of the elementary layer of thickness dx is given as:

$$dR_g = \frac{\rho dx}{A} \tag{3}$$

$$A = Lx\theta \tag{4}$$

After substituting (4) in to (3) and integrating:

$$\int dR_g = \frac{\rho}{L\theta}\int_r^t \frac{1}{x}dx \tag{5}$$

$$R_g = \frac{\rho}{L\theta}\left[\ln x\right]_r^t = \frac{\rho}{L\theta}\ln\left(\frac{t}{r}\right) \tag{6}$$

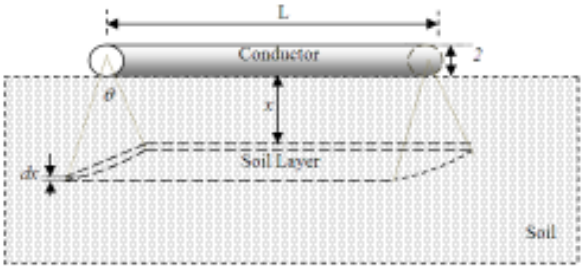

Fig. 3: Schematic diagram of fallen conductor touching the soil

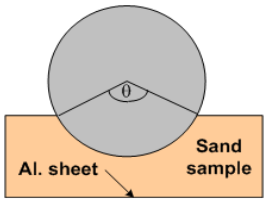

Fig. 4: Schematic diagram of contact angle (θ) with soil layer

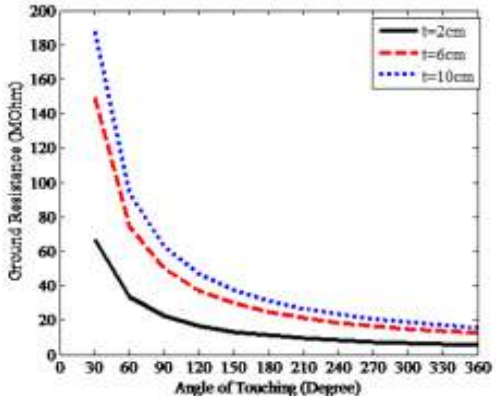

Fig. 5: Variation in R_g with contact angle (θ)

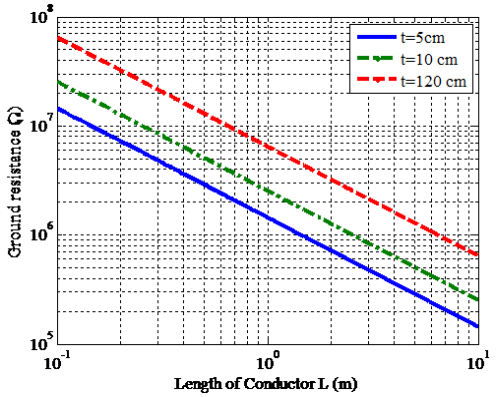

Fig. 6: Variation in R_g with conductor Length (L)

A conductor of length $L = 1.4$ m having radius $r = 8.3$ mm was used in calculating the sand layer's resistance. The resistivity of the sand sample was taken from Table 3 as $\rho = 12.74\times10^6$ Ω-m. It is assumed that the conductor is just touching the sand layer with $\theta = 0.29$ rad (Approx.). The corresponding calculated and the measured values of the sand layer resistance are given in Table 3.

Effect of contact angle on resistance (R_g): Figure 4 shows a schematic diagram of the conductor touching the sand underneath. In this case, the contact angle may change from say about 30° (just touching) to 360° (completely buried) and the corresponding R_g is calculated using Eq. (3) above while keeping all other parameters as mentioned earlier. The variations in

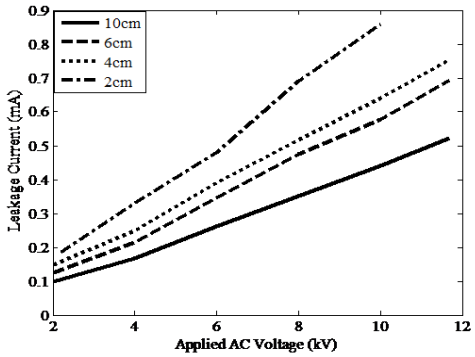

Fig. 7: Variation of leakage current under HVAC

R_g versus θ for different sand layer thicknesses are shown in Fig. 5. This figure clearly shows that the fault resistance decreases with the increase in contact angle. However, the value of this resistance is of the order of MΩ. The main reason for this extremely high value of fault resistance is extremely high resistivity of loose drifting desert sand.

Effect of conductor length on Resistance (R_g): The fault current will depend upon the length of conductor in contact with sand since R_g is inversely proportional to L. The variation of R_g with L for a conductor with just in contact with sand is shown in Fig. 6. If the length of fallen conductor touching the soil is less than the soil thickness, the value of R_g is more and decreases with the increase L. It is clear that even for a 100 m conductor fallen on a small sand thickness layer on a perfectly conducting soil will produce fault resistance of more than 10 kΩ, results in fault current of less than 1A which makes it almost impossible to discriminate the fault.

Fault current measurements: The variation of leakage current versus AC applied voltage for different sand layer thicknesses is shown in Fig. 7. When 8 kVrms is applied, the measured values of current for sand layer thicknesses of 10, 6, 4 and 2 cm are 352, 474, 518 and 690 μA, respectively. The values of current in this case are a bit more than under HVDC. When 8kV DC is applied, the measured values of the currents for the above mentioned sand layer thicknesses are 31.4, 47, 62, 90 and 175 μA, respectively. The value of fault current depends upon the sand layer thickness and as expected, an increase in this thickness reduces the fault current and vice versa. The leakage current magnitudes measured under different applied AC voltages for different thicknesses of sand layers are shown in Table 4. From these results, it is clear that even for a few cm thick sand layer above a perfect conducting ground, the fault current is too low for reliable operation of conventional system protection devices.

From the above discussion it is clear that for each sample thickness, the magnitude of leakage current under DC is always less than the magnitude of the

Table 4: Leakage current I_g (μA) under HVAC

Applied voltage (kV_{rms})	Thickness of the sand layer			
	2 cm	4 cm	6 cm	10 cm
2	0.186	0.148	0.125	0.098
4	0.330	0.249	0.214	0.166
6	0.480	0.391	0.345	0.262
8	0.690	0.518	0.474	0.352
10	0.860	0.642	0.578	0.440
12	1.060	0.754	0.694	0.522

Leakage current under AC. This is due to the presence of charging currents under AC.

The waveforms of the current flowing through the 50 Ω detection resistance were recorded using 300 MHz bandwidth oscilloscope (Model: Tektronic-320) for the following two cases:

i) Leakage current waveform produced when a high voltage conductor had already fallen on ground and was in contact with the sand layer and a voltage was applied.
ii) Leakage current waveforms at the instant when an energized high voltage conductor breaks, falls and comes in contact with the sand layer.

The current oscillographs for the above mentioned two cases are shown in Fig. 8 for a applied voltage of 12 kV. Almost similar leakage current waveforms were obtained for other applied voltages and/or sand layer thicknesses. These waveforms were taken under the same conditions in different attempts for both cases. In case (ii) above, the conductor was dropped while the high voltage applied was "ON" and the instantaneous current flow through the 50 Ω resistance was captured.

Simulation study: The effect of high earth resistance on fault current was analyzed using the simulation setup

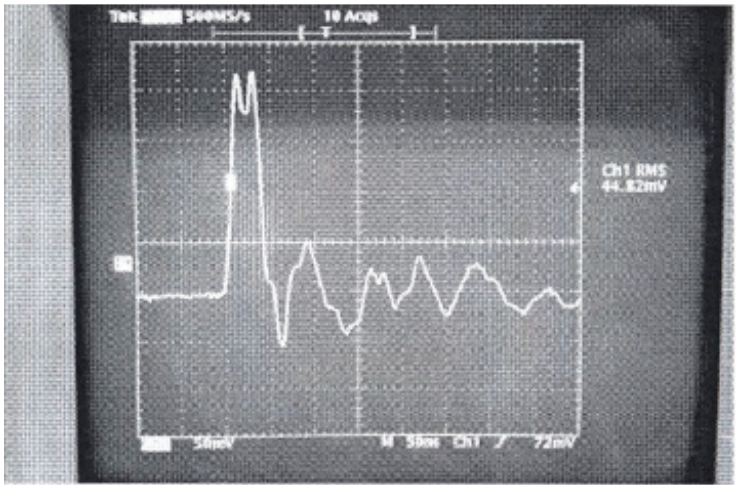

(a) Already fallen open conductor on the sand (sand layer thickness = 5 cm)

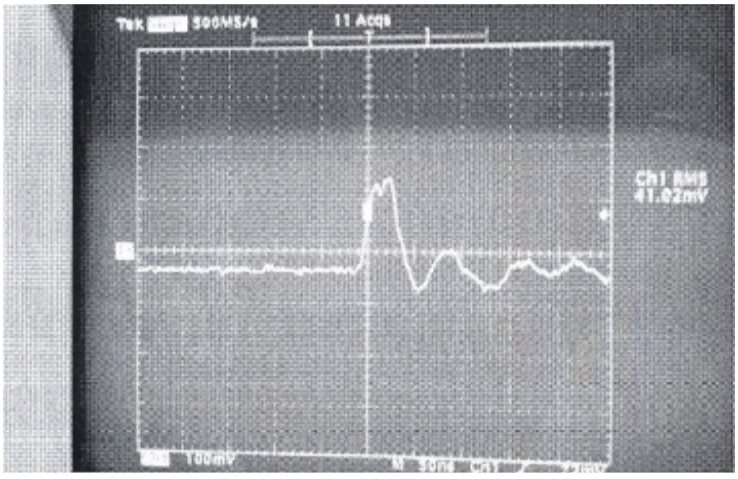

(b) Energized falling conductor at the instant it comes in contact with the soil (sand layer thickness = 8 cm)

Fig. 8: Current oscillgraphs for the broken conductor, (voltage applied: 12 kV)

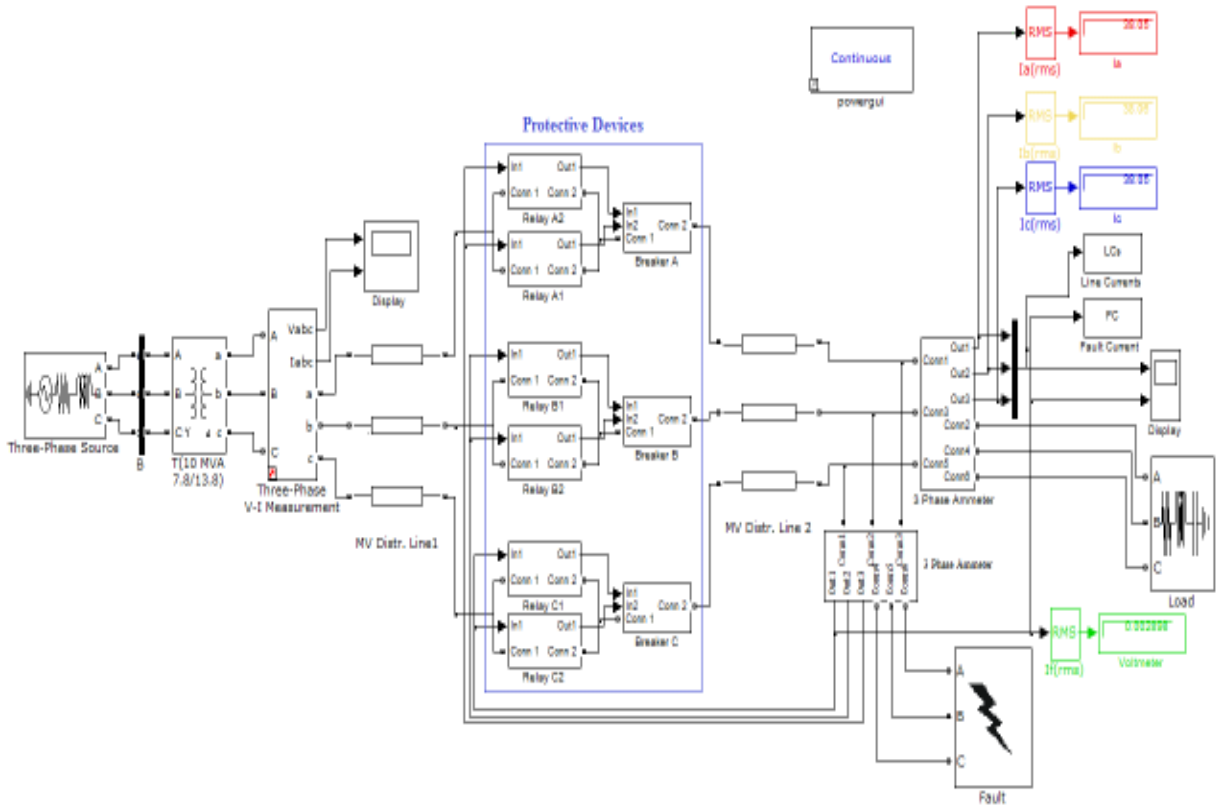

Fig. 9: Simulation circuit with protective devices under simulated HIF condition

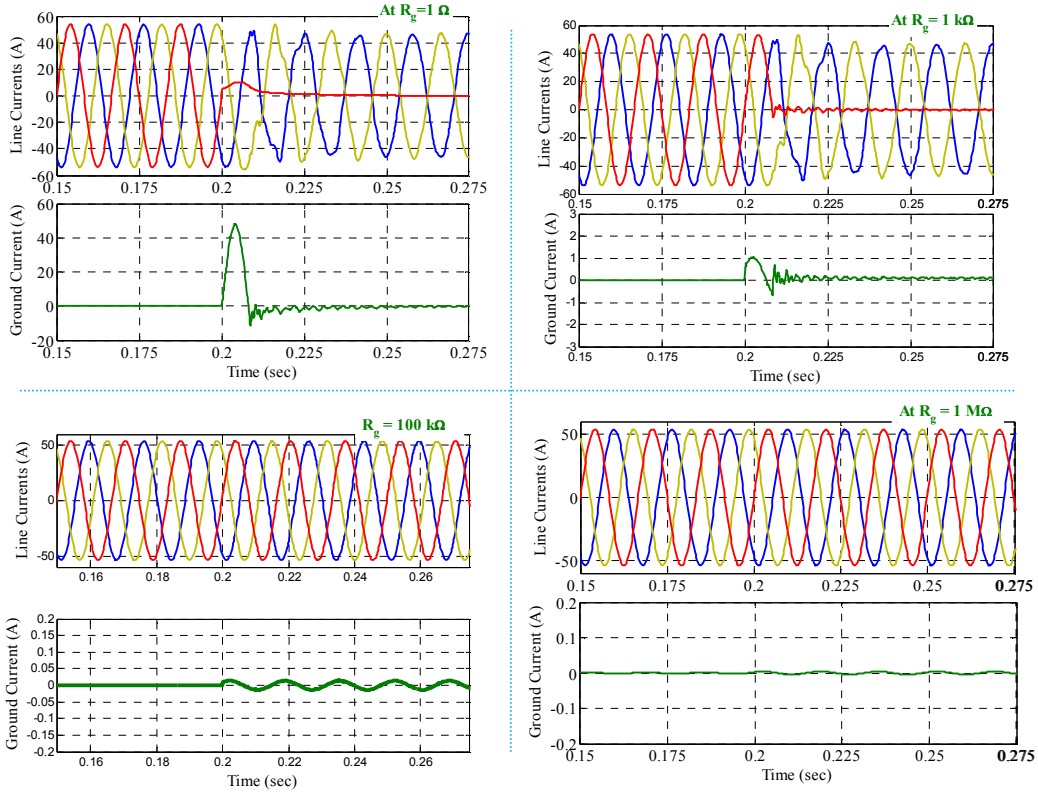

Fig. 10: Simulated current oscillograms under different HIF conditions

Table 5: Variations in the ground fault current with ground fault resistances

Ground resistance (Ω)	Line current (A)			Fault current (A)	Sequence current (A)		
	I_a	I_b	I_c		I_0	I_1	I_2
Case A: open conductor							
1	37.67	39.25	39.40000	39.40000	38.7730	0.5530	0.55300
10	38.19	38.71	39.32000	39.32000	38.7400	0.3270	0.32700
100	42.26	33.10	37.30000	37.30000	37.5530	2.6470	2.64700
1K	40.65	25.29	12.92000	12.92000	26.2870	8.0210	8.02100
10K	34.64	31.79	1.39500	1.39500	22.6080	10.6390	10.63900
1M	33.85	32.66	0.01399	0.01399	22.1750	11.0860	11.08600
100M	33.81	32.65	0.00014	0.00014	22.1530	11.0820	11.08200
Case B: sagging conductor							
1	37.67	39.25	39.39000	37.79000	38.7700	0.5515	0.55154
10	37.95	38.86	39.19000	26.94000	38.6667	0.3708	0.37083
100	38.09	38.21	38.37000	6.30000	38.2233	0.0811	0.08110
1K	38.06	38.08	38.09000	0.71300	38.0767	0.0088	0.00880
10K	38.06	38.07	38.06000	0.07224	38.0633	0.0033	0.00330
1M	38.06	38.06	38.06000	0.000724	38.0600	0	0
100M	38.06	38.06	38.06000	0.00000724	38.0600	0	0

shown in Fig. 9. Initially, the simulations were carried out for 20 km long MV feeder with a 13.8 kV generator on the sending end and 10 MVA balanced load of 0.8 lagging power factor on the receiving end. The ground fault currents in phase-C for different values of earth resistances are given in Table 5 for open (broken) conductor (Table 5 case A) as well as sagging conductor touching the ground (Table 5 case B). As expected, with increase in grounding resistance, the ground fault current decreases. Moreover, when the grounding resistance is more than 10 kΩ, it does not affect the value of line current appreciably. The value of fault current is very small when ground fault resistance values are of the order of MΩ. Hence such situations cannot be detected by conventional protective devices that are based on current measurements.

Moreover, the simulation setup was modified by including proper protective devices as shown in Fig. 9. Setting of the relays were made such that, if the fault current through the ground resistance (R_g) is more than 15 mA, the relay can trip the circuit breaker connected to the faulted line to open it. Figure 10 shows the values of line and fault currents corresponding to different values of fault resistance R_F. When a fault occurred at 0.2 sec, the faulted line got isolated if the value of R_F is of the order of kΩ. However, when the value of R_F is in MΩ range, the ground current is almost zero and circuit breaker remains closed. It has been found that the threshold resistance R_F to detect fault current is about 93 kΩ.

From the above experimental as well as simulation results depicted in Fig. 8 and 10, respectively, it is clear that desert sand sample do not conduct much due to extremely high resistivity of sand which behaves as an insulating material. In KSU, High Voltage Lab, where the above experiments were conducted, the lab grounding resistance is ≤0.5 Ω and thus even very low fault current can be detected. In real desert situation, the grounding resistance at the fault point is expected to be very high and even such small currents will not be noticed. For example, if for 13.8 kV line conductor between the two poles span having about 100 m length breaks and falls on desert sand, assume that sand underneath has $\rho = 12.74\times10^6$ Ω-m and conductor radius is $r = 8.3$ mm, the corresponding $R_g = 488$ GΩ and $I_g = 0.01$ μA. Thus, even if one wants to monitor such transient current through the desert's sand under high voltages, the fault condition cannot be detected using a conventional relaying system and one has to use some innovative techniques based on emerging Smart Grid technologies.

CONCLUSION

This study studies the electrical characteristics of the inland arid desert sand in Saudi Arabia. Different parameters such as soil layer thickness, applied voltage magnitude and type, contact angle of the conductor touching the sand, etc., which can affect the ground resistance and fault current were considered. Based on theoretical and experimental studies the following conclusions are drawn:

- The inland arid desert's sand mainly consists of drifting sand layers and has extremely high electrical resistivity. This leads to very high fault impedance when an energized conductor breaks and falls on such sand.
- The ground resistance decreases with the increase of the conductor contact angle with the sand.
- If a high voltage conductor falls on such sand, then the resulting fault impedance will be very high and there will be negligible fault current. Thus the fault can go undetected by the conventional relaying systems.

The above factors should be considered in order to have proper protection arrangement while designing medium voltage distribution networks that have to operate in such environment.

ACKNOWLEDGMENT

The authors are thankful to the Saudi Aramco Chair in Electrical Power, College of Engineering, King Saud University, Riyadh for technical and financial support of this study.

REFERENCES

Al-Arainy, A.A., N.H. Malik, M.I. Qureshi and Y. Khan, 2011a. Grounding pit optimization using low resistivity materials for applications in high resistivity soils. Int. J. Emerg. Electr. Power Syst., 12: 1-18.

Al-Arainy, A.A., Y. Khan, N.H. Malik and M.I. Qureshi, 2011b. Optimized pit configuration for efficient grounding of the power system in high resistivity soils using low resistivity materials. Proceeding for the 4th International Conference on Modeling, Simulation and Applied Optimization (ICMSAO'11). Kuala Lumpur, Malaysia.

Aucoin, B.M., 1982. Distribution high impedance faults using high frequency current components. IEEE T. Power Deliver., 101(6): 1596-1606.

Aucoin, B.M., 1987. Detection of distribution high impedance faults using burst noise signals near 60Hz. IEEE T. Power Deliver., 2(2): 347-348.

Aucoin, B.M. and R.H. Jones, 1996. High impedance fault detection implementation issues. IEEE T. Power Deliver., 11(1): 139-148.

Callhoun, H., M.T. Bishop, C.H. Eicler and T.E. Lee, 1982. Development and testing of an electro-mechanical relay to detect fallen distribution conductors. IEEE T. Power Ap. Syst., PAS-101(6): 1643-1650.

Craig, G.W., 2001. High Impedance Fault Detection on Distribution Systems. GE Power Management Publications, GER-3993.

David, C., W. Tat and Y. Xia, 1998. A novel technique for high impedance fault detection. IEEE T. Power Deliver., 13(3): 738-741.

Girgis, A.A., W. Chang and E.B. Makram, 1990. Analysis of HIF generated signal using a Kalman filtering technique. IEEE T. Power Deliver., 5(4): 1714-1724.

IEEE PSRC Working Group D15, 2000. High impedance fault detection technology. Report of PSRC. March 1996, Retrieved from: http://grouper.ieee.org/groups/td/dist/documents/highz.pdf.

Jincheng, L. and L.K. Jeffery, 1999. New insight into detection of High Impedance arcing faults on DC trolley system. IEEE T. Ind. Appl., 35(5): 1169-1173.

Khan, Y., N.H. Malik, A.A. Al-Arainy, M.I. Qureshi and F.R. Pazheri, 2010. Efficient use of low resistivity material for grounding resistance reduction in high soil resistivity areas. Proceeding of the IEEE Region 10 Conference on TENCON 2010. Fukuoka, Japan.

Khan, Y., F.R. Pazheri, N. Malik, A.A. Al-Arainy and M.I. Qureshi, 2012. Novel approach of grounding pit optimum dimensions in high resistivity soils. Electr. Pow. Syst. Res., 92: 145-154.

Lai, T.M., L.A. Snider, E. Lo and D. Sutanto, 2005. High-impedance fault detection using discrete wavelet transform and frequency range and RMS conversion. IEEE T. Power Deliver., 20(1): 397-401.

Lee, I., 1982. High impedance fault detection using 3rd harmonic current. EPRI Final Report, EPRI EL-2430.

Russel, B.D., 1988a. An arcing fault detection technique using low frequency current components-performance evaluation using recorded field data. IEEE T. Power Deliver., 3(4).

Russel, B.D., 1988b. Behavior of low frequency spectra during arcing faults and switching events. IEEE T. Power Deliver., 3(4).

Salam, M.A., 2012a. Grounding resistance measurement by grid electrode in Brunei Darussalam. Int. J. Energ. Technol. Policy, 8(2): 196-206.

Salam, M.A., 2012b. Grounding resistance measurement using vertically driven rods near residential areas. Int. J. Pow. Energ. Convers., 4(3).

Salam, M.A. and H. Morsidi, 2010. Grounding resistance measurement by U-shape and square grids. Proceeding of the IEEE International Conference on TENCON 2010. Fukuoka, Japan, T1-11-5: 102-105.

Salam, M.A. and M. Noh, 2012. Measurement of grounding resistance with square grid and rods near substations. Proceeding of the IEEE Electrical Power and Energy Conference (EPEC, 2012). London, Ontario, pp: 134-138.

Samantaray, S.R., B.K. Panigrahi and P.K. Dash, 2008. High impedance fault detection in power distribution networks using time-frequency transform and probabilistic neural network. IET Gener. Transm. Dis., 2(2): 261-270.

Senger, E.C., W. Kaiser, J.C. Santos and P.M.S. Burt, 2000. Broken conductors protection system using carrier communication. IEEE T. Power Deliver., 15(2): 525-530.

Sultan, A.F. and G.W. Swift, 1994. Detecting arcing downed wires using fault current flicker and half cycle asymmetry. IEEE T. Power Deliver., 9(1).